Published in final edited form as:

Stem Cells. 2016 April ; 34(4): 960–971. doi:10.1002/stem.2260.

SCO2 mediates oxidative stress-induced glycolysis to OXPHOS switch in hematopoietic stem cells

Wei Du[1], **Surya Amarachintha**[1], **Andrew F. Wilson**[1], and **Qishen Pang**[1,2]

[1]Division of Experimental Hematology and Cancer Biology, Cincinnati Children's Hospital Medical Center, Cincinnati, Ohio 45229

[2]Department of Pediatrics, University of Cincinnati College of Medicine, Cincinnati, Ohio 45229

Abstract

Fanconi anemia (FA) is an inherited bone marrow (BM) failure syndrome, presumably resulting from defects in hematopoietic stem cells (HSCs). Normal HSCs depend more on glycolysis than on oxidative phosphorylation (OXPHOS) for energy production. Here we show that FA HSCs are more sensitive to the respiration inhibitor NaN3 treatment than to glycolytic inhibitor 2-DG, indicating more dependence on OXPHOS. FA HSCs undergo glycolysis-to-OXPHOS switch in response to oxidative stress through a p53-dependent mechanism. Metabolic stresses induce upregulation of p53 metabolic targets in FA HSCs. Inactivation of p53 in FA HSCs prevents glycolysis-to-OXPHOS switch. Furthermore, p53-deficient FA HSCs are more sensitive to 2-DG-mediated metabolic stress. Finally, oxidative stress-induced glycolysis-to-OXPHOS switch is mediated by SCO2. These findings demonstrate p53-mediated OXPHOS function as a compensatory alteration in FA HSCs to ensure a functional but mildly impaired energy metabolism and suggest a cautious approach to manipulating p53 signaling in FA.

Keywords

Fanconi anemia; hematopoietic stem cells; glycolysis; OXPHOS; p53; SCO2

Introduction

Hematopoietic stem cells (HSCs) are a distinct population of pluripotent cells that can self-renew and differentiate into various types of cells of the blood lineage [1]. Under steady physiological conditions, the most primitive HSCs are in a quiescent state and reside in the bone marrow (BM) niche where they preserve the capacity to self-renew and to continue to produce all types of blood cells throughout a prolonged life span without depleting the

Address correspondence to: Qishen Pang, Division of Experimental Hematology and Cancer Biology, Cincinnati Children's Hospital Medical Center, 3333 Burnet Avenue, Cincinnati, Ohio 45229. Phone: (513) 636-1152. Fax: (513) 636-3768. Qishen.pang@cchmc.org or Wei Du, Division of Radiation Health, College of Pharmacy, UAMS, 4301 W Markham, Little Rock, Arkansas 72205. Phone: (501)-526-6990. wdu@uams.edu.

Authorship

Contribution: W. D., designed research, performed research, analyzed data and wrote the paper; S. A., performed research and analyzed data; A. F. W., performed research; Q. P., designed research, analyzed data and wrote the paper.

Conflict-of-interest disclosure: The authors declare no competing financial interests.

regenerative cell pool [2, 3]. In response to stress or stimulation, the HSCs can move out of the BM niche, enter the cell cycle and undergo division. In addition, the cycling HSCs may return to the BM niche and regain their quiescent state [4]. Disruption of HSC quiescence prematurely exhausts the stem cell pool and causes hematological failure under various stressors, such as oxidative stress, cell cycling, and aging [5, 6]. Like stem cells in other tissues, HSC employs two main modes of energy production: glycolysis and oxidative phosphorylation (OXPHOS). It has recently been demonstrated that HSCs possess a distinct metabolic profile with a preference for glycolysis rather than OXPHOS [7, 8]. However, how HSCs reprogram their metabolism to maintain functions in response to stressors is not well understood.

The tumor suppressor p53 is a master regulator of cell-cycle arrest, apoptosis, senescence, and differentiation, and thus plays a pivotal role in tumorogenesis, cell-death and survival [9, 10]. In addition, p53 is also a central regulator of energy metabolism [11, 12]. p53 regulates energy metabolism at the glycolytic and OXPHOS steps via transcriptional regulation of its downstream genes TP53- induced glycolysis regulator (TIGAR) and synthesis of cytochrome *c* oxidase (SCO2) [13, 14]. On one hand, p53 negatively regulates glycolysis through activation of TIGAR (an inhibitor of the fructose-2,6-bisphosphate). On the other hand, p53 positively regulates OXPHOS through upregulation of SCO2, a member of the COX-2 assembly involved in the electron-transport chain. Recently, it has also been shown that p53 has important functions in hematopoiesis regulating HSC quiescence and self-renewal [15, 16]. Interestingly, how p53 can antagonistically regulate two crucial steps of the energy metabolism and the relation of this regulation with the role of p53 in HSC homeostasis remains to be elucidated.

The ability of HSCs to produce the complete hematopoietic lineages is a major interest in the research of hematopoiesis, and clinically, at the center of stem cell therapy in hematologic diseases including BM failure and leukemia [1, 17]. One of the best studied hematologic disease models is Fanconi anemia (FA), a genetic disorder associated with BM failure, clonal proliferation of hematopoietic stem and progenitor cells, and progression to myelodysplastic syndrome (MDS) and acute myeloid leukemia (AML) [18, 23]. FA is caused by a deficiency in any of the seventeen FA genes (FANCA-Q) [24, 26], which cooperate in a DNA repair pathway for resolving DNA interstrand cross-link (ICL) encountered during replication or generated by DNA-damaging agents [27, 28]. The effect of FA deficiency on energy metabolism in HSC function has yet to be exploited. In this study, we have demonstrated that FA HSCs are more dependent on OXPHOS and undergo the glycolysis to OXPHOS switch in response to oxidative stress to meet the increased demand for energy through a p53-dependent mechanism. We have also identified SCO2 as a critical effector of p53 in mediating the oxidative stress-induced glycolysis to OXPHOS switch. These findings provide novel insights into not only the mechanistic connection between energy deficit and FA HSC defect, but also the beneficial effect of p53 on FA HSC maintenance.

Materials and Methods

Animals

Fanca$^{+/-}$ and *Fancc*$^{+/-}$ mice (C57BL/6: B6, CD45.2^{+}) were provided by Dr. Madeleine Carreau (Laval University) and Dr. Manuel Buchwald (Hospital for Sick Children, University of Toronto), respectively [29, 30]. *p53*$^{-/-}$*Fanca*$^{-/-}$ mice were generated by interbreeding the heterozygous *Fanca*$^{+/-}$ with *p53*$^{+/-}$ mice (C57BL/6: B6, CD45.2^{+}; Jackson Laboratories) [31]. All the animals including BoyJ (C57BL/6: B6, CD45.1^{+}) recipient mice were maintained in the animal barrier facility at Cincinnati Children's Hospital Medical Center. All the animals used for the experiments were 8–12 week-old. All experimental procedures conducted in this study were approved by the Institutional Animal Care and Use Committee of Cincinnati Children's Hospital Medical Center.

Flow analysis and cell sorting

Femurs and tibias were flushed to dissociate the BM fraction. Cells were resuspended in 5mL PBS/0.5% BSA and filtered through a 70-μm filter (BD Biosciences). The mononuclear cells were isolated by Ficoll (GE Healthcare) gradient centrifugation. The following antibodies were used for flow cytometry analyses: APC-Cy7-anti-cKit (Biolegend), PE-Cy7-anti-Sca-1 (BD Biosciences), Pacific blue-anti-CD150 (BioLegend), FITC-anti-CD48, FITC-anti-CD34, PE-anti-CD45.1, APC-anti-CD45.2 (all from BD Biosciences). For lineage labeling, the lineage antibody cocktail included the following biotin-conjugated anti-mouse antibodies: Mac1, Gr-1, Ter119, CD3e, and B220 (BD Biosciences). The secondary reagent used included streptavidin-PerCP-Cy5.5 (BD Biosciences). For LSK (Lineage^{-}Sca-1^{+}c-Kit^{+}) staining, cells were labeled by the biotin-conjugated anti-lineage antibody cocktail followed by staining with a secondary Percp-cy5.5-anti Streptavidin antibody (BD Biosciences), PE-Cy7-anti-Sca-1 antibody (BD Biosciences), and APC-Cy7-anti-cKit antibody (BD Biosciences). To access long-term HSC subpopulation, cells were stained with LSK antibodies in addition to CD150-pacific blue (Biolegend), CD48-FITC (Biolegend) or Alexa fluor 647-anti-CD34 (eBioscience). Flow cytometry was performed on a FACS-LSR II (BD Biosciences) and analysis was done with FACSDiva Version 6.1.2 software (BD Biosciences). For the cell sorting, lineage negative cells were enriched using lineage depletion reagents (StemCell Technologies) according to the manufacturer's instruction. The Lin^{+} or LSK (Lin^{-}/ckit^{+}/Sca-1^{+}) fractions were acquired by using the FACSAria II sorter (BD Biosciences).

Cell culture

Sorted cells were cultured in StemSpan medium (StemCell Technologies) supplemented with 100 ng/ml stem cell factor (SCF), 100 ng/ml TPO (Both were from R&D Systems) and 1% BSA at 37°C in normoxia (21% O_2, 5% CO_2). To investigate the mode of FA HSC energy metabolism under oxidative stress, cells were cultured with 125 μM BSO for 6h or 100 μM of paraquat (Sigma-Aldrich) for 2 h. To test the effect of the glycolytic inhibitor 2-deoxy-Dglucose (2-DG, Sigma-Aldrich) and the respiration inhibitor sodium azide (NaN3, Sigma-Aldrich) on FA HSCs, Low density bone marrow (LDBM) cells were cultured in the presence of indicated doses of 2-DG or NaN3 for 12 hours followed by FACS analysis.

Measurements of glucose, lactate, PK, ATP and OCR

Glucose consumption, lactate production and pyruvate kinase (PK) activity were measured in the culture media using the Glucose Assay Kit, the Lactate Assay Kit and the Pyruvate Kinase Activity Assay Kit (All from Biovision), respectively, according to the manufacturer's instructions. Intracellular ATP levels were determined in cell lysates using the ATP Bioluminescent Somatic Cell Assay Kit (Sigma-Aldrich), following the manufacturer's instructions. Oxygen consumption rate (OCR) was measured in Seahorse 96-well XF Cell Culture Microplates in conjunction with an XF^e96 sensor cartridge (XF^e96 FluxPak mini; Part#102601-100) using XF^e96 Extracellular Flux Analyzer (Seahorse bioscience).

Immunocytochemistry

Sorted $CD34^-LSK$ cells were cytospun onto glass slides, fixed with 4% paraformaldehyde. Slides were incubated with blocking solution (1XPBS / 0.25% Triton X-100 / 5% BSA), and subsequently processed for staining with p53 (Clone PAb240; Calbiochem) primary antibody and Alexa Fluor 488-conjugated Donkey anti-Mouse IgG secondary antibodies (Jackson ImmunoResearch). DNA was stained by using DAPI.

Western blotting

Equal numbers of Lin^- cells isolated from *Fanca*$^{-/-}$, *Fancc*$^{-/-}$, or their WT littermates were washed with ice-old PBS, and resuspended in an ice-cold lysis buffer containing 50mM Tris-HCL (pH7.4), 0.1% NP40, and 1M NaCl supplemented with protease and phosphatase inhibitors (10 μg/ml of aprotinin, 25 μg/ml of leupeptin, 10 μg/mlof pepstatin A, 2mM PMSF, 0.1M NaP2O4, 25mM NaF, and 2mM sodium orthovanadate) for 30 minutes on ice. Cell debris was removed from the lysate by centrifuging them at 16873g for 30 minutes at 4°C. Protein lysate was resolved on SDS-PAGE and transferred onto nitrocellulose membranes. Immunoblots were then incubated with primary antibodies for total p53 (Clone PAb240; Calbiochem), p53-S18 (Clone ab1431; Abcam), and β-actin (Sigma-Aldrich) for 12–16 hours at 4°C. Signals were visualized by incubation with anti-mouse secondary antibody, followed by ECL chemiluminescence (Amersham Biosciences).

Quantitative PCR

Total RNA was prepared with RNeasy kit (Qiagen, Valencia, CA) following the manufacturer's procedure. Reverse transcription was performed with random hexamers and Superscript II RT (Invitrogen, Grand Island, NY) and was carried out at 42 °C for 60 min and stopped at 95 °C for 5 min. First-strand cDNA was used for real-time polymerase chain reaction (PCR) using primers listed in Table S2. Samples were normalized to the level of Glyceraldehyde-3-phosphate dehydrogenase (*Gapdh*) mRNA.

Lentiviral vector construction, virus production and transduction

To generate shRNA vectors against Sco2 or Tigar, oligonucleotides (Table S3) were cloned into the SF-LV-shRNA-EGFP vector (provided by Dr. Lenhand Rudolph, Institute of Molecular Medicine and Max-Planck-Research, Germany) [32]. A nonsense scrambled shRNA sequence was used as a negative control. To generate a lentiviral expression vector

for SCO2, The Sco2 cDNA [33] was amplified from Transomic plasmid TCM1304 (Transomic), and cloned into the pLVX-IRES-GFP vector (Clontech).

Lentivirus was produced in 293 T cells after transfection of 20 μg plasmid, 15 μg pCMVΔ8.91 helper plasmid and 6 μg pMD.G [34] using standard calcium phosphate transfection procedures. Medium was replaced with fresh medium 12 hours after transfection. To harvest viral particles, supernatants were collected 48 hours after transfection, filtered through 0.45 μm-pore-size filters, and concentrated at 25,000rpm for 2.5 hours at 4°C. Virus pellet was resuspended in sterile PBS and stored at −80°C.

For lentivirus transduction, the sorted LSK cells from WT, *p53*$^{-/-}$, *Fanca*$^{-/-}$, and *p53*$^{-/-}$*Fanca*$^{-/-}$ were maintained in StemSpan™ Serum-Free Expansion Media (Stemcell Technologies) with 50 ng/ml SCF and 50 ng/ml TPO (both from Peprotech, Rocky Hill, NJ) for 24 hours before transduction. A multiplicity of infection (MOI) of 10 was used in all shRNA experiments and a MOI of 5 for SCO2 overexpression. Cells were transduced overnight in the presence of 0.5 mg/ml polybrene and re-fed with fresh medium the next day. Transduced cells were used in further assays at least 3 to 4 days post transduction.

Bone Marrow Transplantation

For glycolysis- and OXPHOS-inhibition experiments, Fifty SLAM cells from WT, *Fanca*$^{-/-}$, *Fancc*$^{-/-}$, *p53*$^{-/-}$ or *p53*$^{-/-}$*Fanca*$^{-/-}$ (DKO) mice (CD45.2) were treated with10mM 2-DG or 5mM NaN3 for 12 h, mixed with 4×10^5 BM LDMCs from recipient mice (CD45.1), and transplanted into lethally irradiated BoyJ congenic mice (CD45.1). For NaN3-BSO treatment, fifty WT or FA SLAM cells from WT, *Fanca*$^{-/-}$ or *Fancc*$^{-/-}$ mice (CD45.2) were pre-treated with 5mM NaN3 for 30 min then with 125μM BSO for another 6h, and then transplanted together with 4×10^5 recipient cells into lethally irradiated BoyJ congenic mice. For Sco2- and Tigar-KD and Sco2 over-expression experiments, 1500 transduced LSK cells were treated with 125μM BSO for 6h, and transplanted together with 4×10^5 recipient cells into lethally irradiated BoyJ congenic mice. Six months after transplantation, peripheral blood was collected and examined to determine the percentage of donor-derived cells by FACS.

Statistics

Data was analyzed statistically using a standard t test (Prism v6.0). The level of the statistical significance stated in the text was based on the P values. $P < 0.05$ was considered statistically significant.

Results

FA HSCs are more dependent on OXPHOS for energy metabolism

The mammalian HSCs depend more on glycolysis for energy supply than on OXPHOS and show higher glycolytic capacity than other lineages of BM cells [7, 8]. To determine whether FA deficiency alters HSC energy metabolism, we measured the rates of glycolysis and OXPHOS in HSC-enriched Lin$^-$Sca-1$^+$c-Kit$^+$ (LSK) cells and differentiated hematopoietic cells (Lin$^+$) from the BM of WT or FA (*Fanca*$^{-/-}$ or *Fancc*$^{-/-}$; note that the results with the

Fancc$^{-/-}$ mice are shown in the Supplementary figures) mice (Fig. S1A). Strikingly, deletion of *Fanca* or *Fancc* markedly reduced glucose consumption and lactate production in LSK cells compared to WT controls, while having little effect on Lin^{+} cells (Fig. 1A, B and Fig. S1B, C). Consistently, FA LSK cells produced lower ATP levels than WT cells (Fig. 1C and Fig. S1D). Surprisingly, FA LSK cells also exhibited decreased oxygen consumption levels (Fig. 1D and Fig. S1E). It should be noted that FA Lin^{+} cells also showed decreased ATP and oxygen consumption, albeit not statistically significant, compared to WT controls (Fig. 1C, D and Fig. S1D, E).

The observation described above suggests that the FA HSCs might be unable to turn to OXPHOS for energy provision on deficient glycolysis. To test this notion, we evaluated the effect of the glycolytic inhibitor 2-deoxy-Dglucose (2-DG) and the respiration inhibitor sodium azide (NaN3) on FA HSCs. The presence of 2-DG significantly reduced the absolute number of WT phenotypic HSCs (CD150^{+} CD48^{-} LSK; SLAM) [35, 36] starting at 5 mM compared to an untreated control (Fig. 1E and Fig. S1F). However, FA HSCs appeared to be resistant to the cytotoxicity of 2-DG even up to 40 mM (Fig. 1E and Fig. S1F). Surprisingly, FA HSCs showed hypersensitivity to the cytotoxicity of the respiration inhibitor NaN3, even at a very low concentration (1 mM) (Fig. 1F and Fig. S1G). These results indicate that FA HSCs are more sensitive to the treatment of the respiration inhibitor NaN3 than to that of glycolytic inhibitor 2-DG, and suggest that these FA HSCs are less dependent on glucose metabolism than WT HSCs.

We next performed a competitive repopulation assay to determine the effect of inhibition of glycolysis or OXPHOS on the function of FA HSCs *in vivo*. Fifty WT or FA SLAM cells (CD45.2) treated *ex vivo* with 10 mM 2-DG or 5 mM NaN3, along with 4×10^5 recipient BM cells (CD45.1), were transplanted into lethally irradiated recipient mice (CD45.1). Six months later, the repopulating ability of donor HSCs was assessed by measuring the percentage of donor-derived cells in the peripheral blood of the transplant recipients. WT HSCs showed more sensitivity to the inhibitory effect of 2-DG than to that of NaN3 on hematopoietic repopulation (Fig. 1G and S1H). In contrast, the repopulating ability of *Fanca*$^{-/-}$ or *Fancc*$^{-/-}$ SLAM cells was relatively resistant to the glycolytic inhibitor, but sensitive to OXPHOS inhibition by NaN3 (Fig. 1G and S1H). Taken together, this *in vivo* data further corroborates the notion that FA HSCs are less dependent on glucose metabolism than WT HSCs.

FA HSCs undergo glycolysis to OXPHOS switch in response to oxidative stress

Normal HSCs predominantly use aerobic glycolysis for ATP production, which shuts down OXPHOS even under a high oxygen level, thus preventing ROS generation [7, 8]. To investigate the mode of FA HSC energy metabolism under oxidative stress, we treated WT and *Fanca*$^{-/-}$ or *Fancc*$^{-/-}$ LSK cells with buthionine sulfoximine (BSO), an inhibitor of glutathione synthetase previously shown to experimentally increase intracellular reactive oxygen species (ROS) levels in HSCs [37] or paraquat, a chemical that can induce accumulation of ROS [38] (Fig. 2A). We tested different doses of these two agents for the production of intracellular ROS, and found that BSO at 125 μM for 6h or paraquat at 100 μM for 2 h generated similar levels of ROS not only in WT LSK cells but also in *Fanca*$^{-/-}$

and *Fancc*$^{-/-}$ cells, which showed higher levels of ROS induced by both chemicals than WT cells (Fig 2A). Therefore, we chose these conditions for the experiments described below. Interestingly, we observed an increased glucose consumption (Fig. 2B) and lactate production (Fig. 2C) in BSO- or paraquat-treated WT LSK cells compared to untreated control cells. In contrast, there was a significant reduction of glucose consumption and lactate production in *Fanca*$^{-/-}$ and *Fancc*$^{-/-}$ LSK cells upon BSO or paraquat treatment (Fig. 2B and 2C). Consistently, the activity of pyruvate kinase (PK), which catalyzes an ATP-generating step in glycolysis, was increased in WT LSK cells, but decreased in *Fanca*$^{-/-}$ or *Fancc*$^{-/-}$ LSK cells under oxidative stress (Fig. 2D). Thus, it is possible that a decreased level of PK activity may be responsible for the observed reduction in glucose consumption and lactate production in *Fanca*$^{-/-}$ and *Fancc*$^{-/-}$ LSK cells. Surprisingly, BSO or paraquat treatment significantly increased ATP production in *Fanca*$^{-/-}$ and *Fancc*$^{-/-}$ LSK cells, although the levels of intracellular ATP in these FA LSK cells were still significantly lower than WT cells at both basal and stressed conditions (Fig. 2E). Significantly, we observed FA LSK cells displayed increased mitochondria oxygen consumption under oxidative stress compared to untreated conditions (Fig. 2F).

The observation that BSO treatment decreased glycolysis, but increased oxygen consumption and ATP production in FA HSCs suggests that these FA HSCs might be more dependent on OXPHOS for energy demand in response to oxidative stress. To test this hypothesis, we examined the effect of OXPHOS inhibition on energy metabolism of FA HSCs under oxidative stress. Addition of the OXPHOS inhibitor, NaN3, completely abrogated the elevated ATP synthesis induced by BSO (Left) or paraquat (Right) in FA LSK cells (Fig. 2G and S2A), indicative of the contribution of mitochondria OXPHOS to the total ATP production. Moreover, NaN3 caused no significant change in BSO- or paraquat-treated WT LSK cells (Fig. 2F and S2A); further confirming that ATP production in WT LSK cells came primarily from glycolysis under both basal and stressed conditions. Consistently, NaN3 further decreased the frequency and repopulating capacity of FA, but not WT HSCs (Fig. 2H, I and S2B, C). Taken together, these results suggest that in response to oxidative stress, FA HSC/progenitor cells switch their energy metabolism from aerobic glycolysis to OXPHOS.

p53 is upregulated in FA HSCs in response to metabolic stress

The observation that FA HSCs undergo a glycolysis to OXPHOS switch in response to oxidative stress prompted us to investigate the underlying molecular mechanism. Q-PCR analysis of the major regulators of glycolysis and OXPHOS revealed that deletion of *Fanca* or *Fancc* in SLAM cells upregulated basal and BSO-induced expression of the p53 target genes synthesis of cytochrome c oxidase 2 (*Sco2*), a component of COX, the main cellular site of oxygen utilization [13, 14], and TP53-induced glycolysis and apoptosis regulator (*Tigar*), a negative regulator of glycolysis (Fig. 3A and Table S1) [13]. In contrast, several p53-repressed genes involved in glycolysis, including those encoding the glucose transporters Glut1, Glut3 and Glut4 [39–41], and the glycolytic enzyme phosphoglycerate mutase 2 (Pgam2) [42], were downregulated (Fig. 3A and Table. S1). Two other p53 metabolic targets, guanidinoacetate methyl transferase (Gamt) [43], and glutaminase 2 (Gls2) [44], were unaffected (Fig. 3A and Table. S1).

Because p53 is a major regulator of energy metabolism [11, 12] and because the p53 pathway plays important roles in FA BM failure and tumorigenesis [45–48], we investigated the engagement of p53 in a metabolic stress response in FA Lin$^-$ cells, a population enriched for hematopoietic stem and progenitor cells (HSPCs). We observed a dose-dependent increase in the expression of total and phosphorylated p53 in both WT and *Fanca*$^{-/-}$ or *Fancc*$^{-/-}$ HSPCs upon BSO or NaN3 treatment (Fig. 3B, C). However, it appeared that *Fanca*$^{-/-}$ or *Fancc*$^{-/-}$ cells displayed much higher and prolonged p53 upregulation compared to WT cells (Fig. 3B, C). Similar results were obtained from p53 immunofluorescence staining of CD34$^-$LSK cells, a population consisting mostly of phenotypic HSCs isolated from the BM of WT and *Fanca*$^{-/-}$ mice (Fig. 3D, E). These results indicate that p53 is upregulated in FA HSPCs in response to metabolic stress and suggest that p53 may be a crucial regulator in the bioenergetic pathway controlling adaptation to metabolic stress in FA HSPCs.

Oxidative stress mediates glycolysis to OXPHOS switch in FA HSCs via p53 signaling

To further define the role of p53 in FA HSC energy metabolism, we deleted the *p53* gene in *Fanca*$^{-/-}$ mice. p53 deficiency significantly increased glucose consumption and lactate production in both WT (*p53*$^{-/-}$ group) or *Fanca*$^{-/-}$ (DKO group) LSK cells treated with or without BSO (Fig. 4A, B), consistent with the regulatory role of p53 on glucose metabolism. *p53*-deficient *Fanca*$^{-/-}$ (DKO) LSK cells also exhibited increased ATP production and decreased oxygen consumption, compared to *p53*-suficient *Fanca*$^{-/-}$ LSK cells, under both steady and oxidative stress conditions (Fig. 4C, D). These results indicate that the p53 signaling prevents *Fanca*$^{-/-}$ HSPCs from reprogramming to aerobic glycolysis.

We next assessed the functional consequence of p53 deficiency on FA HSC energy metabolism by determining the ability of p53-deficient *Fanca*$^{-/-}$ HSCs to turn to OXPHOS for energy provision on glycolytic inhibition. First, we evaluated the effect of p53 deficiency on the glycolytic inhibitory effect of 2-DG by measuring the frequencies of SLAM cells in cultured LSK cells after 10 mM 2-DG treatment. Remarkably, 2-DG treatment induced severe depletion of p53-deficient *Fanca*$^{-/-}$ SLAM cells (Fig. 4E). In contrast, the frequency of p53-suficient *Fanca*$^{-/-}$ SLAM cells was virtually unaffected (Fig. 4E). We next determined the *in vivo* effect of p53 deficiency on the glycolytic inhibitory effect of 2-DG by analyzing the competitive repopulation of LSK cells in lethally irradiated transplant recipients after *ex vivo* treatment with 10 mM 2-DG. Six months after BM transplantation, 12 h of 2-DG exposure decreased repopulation of p53-deficient *Fanca*$^{-/-}$ (DKO) LSK cells significantly more than that of p53$^{-/-}$ or WT LSK cells (96.1% decrease in DKO vs 68.2% and 21.3% decrease in *p53*$^{-/-}$ and WT groups, respectively; Fig. 4F). The ability of repopulation in 2-DG-treated p53-suficient *Fanca*$^{-/-}$ LSK cells, however, did not show a significant decrease compared to that of the untreated cells at 6 months after transplantation (Fig. 4F). This data indicates that p53 deficiency in FA HSCs results in an increase in dependence on glycolysis for energy provision with a consequently higher sensitivity to 2-DG.

Oxidative stress-induced glycolysis to OXPHOS switch is mediated by SCO2

We then made effort to identify the effector of p53 signaling in controlling the oxidative stress-induced glycolysis to OXPHOS switch in FA HSCs. Because BSO treatment upregulated SCO2, which stimulates OXPHOS [14] and TIGAR that functions to suppress glycolysis [13], in *Fanca*$^{-/-}$ and *Fancc*$^{-/-}$ SLAM cells (Fig. 3A and Table. S1), we focused on these two p53 metabolic targets. We first used lentivirally expressed shRNAs to knockdown murine *Sco2* and *Tigar* in WT and *Fanca*$^{-/-}$ BM LSK cells and sorted for GFP^{+} cells. We achieved a greater than 70% reduction in mRNA expression for both *Sco2* and *Tigar* genes (Fig. S3A). The sorted GFP^{+}LSK cells were subjected to further analysis for oxidative stress-mediated OXPHOS and *in vivo* hematopoietic repopulation. Knocking down (KD) *Sco2* significantly reduced both basal and BSO-induced oxygen consumption in *Fanca*$^{-/-}$ GFP^{+}LSK cells (Fig. 5A), suggesting that upregulation of Sco2 by p53 may be one mechanism for the switch from glycolysis to OXPHOS in FA HSCs. In contrast, depletion of Tigar resulted in no significant decrease in oxygen consumption in both untreated and BSO-treated *Fanca*$^{-/-}$ GFP^{+}LSK cells (Fig. S3B), indicating that upregulation of this p53 metabolic target cannot account for the OXPHOS switch in these cells. Similar results were obtained with competitive repopulation assays, in which Sco2-KD decreased repopulation of *Fanca*$^{-/-}$ LSK cells significantly more than that of Sco2-depleted WT LSK cells 6 months after BM transplantation (78.4% decrease in *Fanca*$^{-/-}$ Sco2-KD vs 35.2% decrease in WT Sco2-KD; Fig. 5B). In contrast, the ability of repopulation of Tigar-depleted *Fanca*$^{-/-}$ LSK cells, as well as Tigar-depleted WT LSK cells, did not show any significant decrease compared to that of the control shRNA-transduced LSK cells at 6 months after transplantation (Fig. S3C). Furthermore, ectopic expression of Sco2 (Fig. S3D) almost completely restored BSO-induced oxygen consumption (Fig. 5C) and long-term hematopoietic repopulation (Fig. 5D) of p53$^{-/-}$ or p53-deficient *Fanca*$^{-/-}$ (DKO) LSK cells. Taken together, this data indicates that SCO2 is at least one of the p53 effectors mediating the oxidative stress-induced glycolysis to OXPHOS switch in FA HSCs.

Discussion

Emerging evidence has revealed that resting quiescent HSCs use primarily anaerobic glycolysis for energy production and this metabolic program is required to maintain HSC function [7, 8, 49]. However, HSCs may undergo metabolic reprogramming when they exit the quiescent state in response to a rising energy demand under conditions of stressors or even differentiation. The current study provides evidence that reprogramming from a glycolytic to oxidative metabolism occurs during an HSC's response to oxidative stress. We have utilized the FA model, in which BM failure or leukemia develops as a consequence of HSC defects [18, 21, 23], to demonstrate that this reprogramming is essential for HSC maintenance, and that the p53/SCO2-dependent metabolic pathway regulates this critical metabolic transition.

Surprisingly, FA HSCs are more dependent on OXPHOS in their resting state and undergo a glycolysis to OXPHOS switch in response to oxidative stress. We proposed that these effects were mediated by p53. This was supported by the observations that metabolic stressors, in the forms of ROS induced by BSO or OXPHOS inhibition by NaN3 treatment, induced

upregulation of p53 and its metabolic targets in FA HSCs. Genetically, we defined unambiguously, the role of p53 in metabolic reprogramming by showing that inactivation of p53 in FA HSCs prevented the glycolysis to OXPHOS switch. Moreover, we showed functionally, that p53-deficient FA HSCs turn to glycolysis for energy provision. Because p53 deficiency renders FA HSCs more sensitive to 2-DG treatment than p53-sufficient FA HSCs, the observed decrease in the repopulating capacity of 2-DG-treated DKO LSKs is most likely due to an impaired HSC potential of these cells or to a loss of the SLAM population (Fig. 4E and 4F). This data is consistent with the well-established role of p53 in metabolism; that is, it increases aerobic metabolism and inhibits glycolysis [11, 12].

Several recent studies using mouse models suggest a critical role for p53 in HSC self-renewal and quiescence [50–54] and precise regulation of p53 activity is likely to be important in determining the response of HSCs to not only genotoxic and oncogenic stress, but also to metabolic stress. In the context of FA, emerging evidence suggests that p53 deficiency may increase cancer development in patients with FA and FA mice [45–47]. Conversely, recent studies show that overactive p53 could cause HSPC depletion in the BM of FA patients [48]. Our findings described here add another facet to the function of this tumor suppresser: p53-mediated OXPHOS function as a compensatory alteration in FA HSCs to ensure a functional, but suboptimal energy metabolism.

We identified SCO2 as the effector mediating the p53-dependent oxidative stress-induced glycolysis to OXPHOS switch. Knocking down Sco2 significantly reduced both oxygen consumption and hematopoietic repopulation of *Fanca*$^{-/-}$ GFP^{+}LSK cells treated with the ROS producer BSO. Conversely, ectopic expression of SCO2 restored BSO-induced oxygen consumption and long-term hematopoietic repopulation of BSO-treated p53-deficient *Fanca*$^{-/-}$ LSK cells. Since *Sco2* is a p53 target gene, it is conceivable that the deletion of p53 in FA HSCs depletes Sco2, which positively regulates OXPHOS [54]. Because FA HSCs tend to turn to OXPHOS for energy provision, knockdown of Sco2 would inhibit the repopulating activity of FA HSCs. On the other hand, overexpression of Sco2 in DKO HSCs would enhance their repopulating capacity. It is also known that p53 regulates glycolysis through transactivation of TIGAR [55]. Our gene expression analysis showed that BSO treatment also upregulated TIGAR, which can conceivably mediate the switch by suppressing glycolysis, thereby shifting the balance towards OXPHOS. However, our knock-down experiments showed that depletion of TIGAR did not lead to a decrease in oxygen consumption or long-term hematopoietic repopulation of BSO-treated *Fanca*$^{-/-}$ GFP^{+}LSK cells, indicating that upregulation of this p53 metabolic target was not responsible for the OXPHOS switch in these cells. Thus, these findings support a model whereby oxidative stress upregulates p53, which induces the glycolysis to OXPHOS switch in part by orchestrating a SCO2-mediated mechanism for HSC maintenance. How p53 can antagonistically regulate two crucial steps of energy metabolism and the relevance of this regulation to its well-defined tumor suppressor role remains to be elucidated.

Together, the current study suggests that a metabolic transition that suppresses glycolysis and favors OXPHOS is an essential component of metabolic reprogramming that HSCs, particularly FA HSCs, employ to meet an increase in energy demand under oxidative stress. In addition, our data provides novel information on the function of p53, previously shown as

over activated in FA HSCs, representing a new paradigm in HSC energy metabolism and cautioning that targeting p53 in FA, while potentially eliciting temporary growth improvement, might have the unanticipated detrimental consequence of increasing the long-term risk of HSC defect.

Supplementary Material

Refer to Web version on PubMed Central for supplementary material.

Acknowledgments

We thank Dr. Madeleine Carreau (Laval University) for *Fanca*$^{+/-}$ mice and Dr. Manuel Buchwald (University of Toronto) for *Fancc*$^{+/-}$ mice, Dr. Lenhand Rudolph, Institute of Molecular Medicine and Max-Planck-Research, Germany for SF-LV-shRNA-EGFP vector, Dr. Xiaoli Li for technical assistance, Ms. Danielle Davis for reviewing the manuscript, and the Comprehensive Mouse and Cancer Core of the Cincinnati Children's Research Foundation (Cincinnati Children's Hospital Medical Center) for bone marrow transplantation service. This investigation was supported by NIH grants R01 HL076712, R01 CA157537 and T32 HL091805. Q.P. is supported by a Leukemia and Lymphoma Scholar award.

References

1. Orkin SH, Zon LI. Hematopoiesis: an evolving paradigm for stem cell biology. Cell. 2008; 132:631–644. [PubMed: 18295580]
2. Morrison SJ, Uchida N, Weissman IL. The biology of hematopoietic stem cells. Annu Rev Cell Dev Biol. 1995; 11:35–71. [PubMed: 8689561]
3. Orford KW, Scadden DT. Deconstructing stem cell self-renewal: genetic insights into cell-cycle regulation. Nat Rev Genet. 2008; 9:115–128. [PubMed: 18202695]
4. Wilson A, Trumpp A. Bone-marrow hematopoietic-stem-cell niches. Nat Rev Immunol. 2006; 6:93–106. [PubMed: 16491134]
5. Cheng T, Rodrigues N, Shen H, et al. Hematopoietic stem cell quiescence maintained by p21$^{cip1/waf1}$. Science. 2000; 287:1804–1808. [PubMed: 10710306]
6. Hock H, Hamblen MJ, Rooke HM, et al. Gfi-1 restricts proliferation and preserves functional integrity of haematopoietic stem cells. Nature. 2004; 431:1002–1007. [PubMed: 15457180]
7. Simsek T, et al. The distinct metabolic profile of hematopoietic stem cells reflects their location in a hypoxic niche. Cell Stem Cell. 2010; 7(3):380–390. [PubMed: 20804973]
8. Takubo K, Kocabas F, Zheng J, et al. Regulation of glycolysis by Pdk functions as a metabolic checkpoint for cell cycle quiescence in hematopoietic stem cells. Cell Stem Cell. 2013; 12(1):49–61. [PubMed: 23290136]
9. Vogelstein B, Lane D, Levine AJ. Surfing the p53 network. Nature. 2000; 408:307–310. [PubMed: 11099028]
10. Liebermann DA, Hoffman B, Vesely D. p53 induced growth arrest versus apoptosis and its modulation by survival cytokines. Cell cycle. 2007; 6:166–170. [PubMed: 17264673]
11. Jones RG, Thompson CB. Tumor suppressors and cell metabolism: a recipe for cancer growth. Genes Dev. 2009; 23:537–548. [PubMed: 19270154]
12. Vousden KH, Ryan KM. p53 and metabolism. Nat Rev Cancer. 2009; 9:691–700. [PubMed: 19759539]
13. Bensaad K, Tsuruta A, Selak MA, et al. TIGAR, a p53-inducible regulator of glycolysis and apoptosis. Cell. 2006; 126:107–120. [PubMed: 16839880]
14. Matoba S, Kang JG, Patino WD, et al. p53 regulates mitochondrial respiration. Science. 2006; 312:1650–1653. [PubMed: 16728594]
15. Asai T, Liu Y, Bae N, Nimer SD. The p53 tumor suppressor protein regulates hematopoietic stem cell fate. J Cell Physiol. 2011; 226(9):2215–2221. [PubMed: 21660944]

16. Nii T, Marumoto T, Tani K. Roles of p53 in various biological aspects of hematopoietic stem cells. J Biomed Biotechnol. 2012; 2012:903435. [PubMed: 22778557]
17. Felfly H, Haddad GG. Hematopoietic stem cells: potential new applications for translational medicine. J Stem Cells. 2014; 9(3):163–197. [PubMed: 25157450]
18. Bagby GC Jr. Genetic basis of Fanconi anemia. Curr Opin Hematol. 2003; 10:68–76. [PubMed: 12483114]
19. Alter BP, Giri N, Savage SA, et al. Malignancies and survival patterns in the National Cancer Institute inherited bone marrow failure syndromes cohort study. Br J Haematol. 2010; 150:179–188. [PubMed: 20507306]
20. Kee Y, D'Andrea AD. Expanded roles of the Fanconi anemia pathway in preserving genomic stability. Genes Dev. 2010; 24:1680–1694. [PubMed: 20713514]
21. Soulier J. Fanconi Anemia. ASH Education Program Book. 2011; 1:492–497.
22. Tischkowitz M, Dokal I. Fanconi anaemia and leukaemia - clinical and molecular aspects. Br J Haematol. 2004; 126:176–191. [PubMed: 15238138]
23. Wilson DB, Link DC, Mason PJ, Bessler M. Inherited bone marrow failure syndromes in adolescents and young adults. Ann Med. 2014:1–11.
24. Kee Y, D'Andrea AD. Molecular pathogenesis and clinical management of Fanconi anemia. J Clin Invest. 2012; 122:3799–3806. [PubMed: 23114602]
25. Walden H, Deans AJ. The Fanconi anemia DNA repair pathway: structural and functional insights into a complex disorder. Annu Rev Biophys. 2014; 43:257–278. [PubMed: 24773018]
26. Wang AT, Smogorzewska A. SnapShot: Fanconi anemia and associated proteins. Cell. 2015; 160(1–2):354–354. [PubMed: 25594185]
27. Deans AJ, West SC. DNA interstrand crosslink repair and cancer. Nat Rev Cancer. 2011; 11:467–480. [PubMed: 21701511]
28. Kottemann MC, Smogorzewska A. Fanconi anaemia and the repair of Watson and Crick DNA crosslinks. Nature. 2013; 493:356–363. [PubMed: 23325218]
29. Wong JC, Alon N, Mckerlie C, Huang JR, Meyn MS, Buchwald M. Targeted disruption of exons 1 to 6 of the Fanconi Anemia group A gene leads to growth retardation, strain-specific microphthalmia, meiotic defects and primordial germ cell hypoplasia. Hum Mol Genet. 2003; 12:2063–2076. [PubMed: 12913077]
30. Chen M, Tomkins DJ, Auerbach W, et al. Inactivation of Fac in mice produces inducible chromosomal instability and reduced fertility reminiscent of Fanconi anaemia. Nat Genet. 1996; 12(4):448–451. [PubMed: 8630504]
31. Jacks T, Remington L, Williams BO, et al. Tumor spectrum analysis in p53-mutant mice. Curr Biol. 1994; 4:1–7. [PubMed: 7922305]
32. Wang J, Sun Q, Morita Y, et al. A differentiation checkpoint limits hematopoietic stem cell self-renewal in response to DNA damage. Cell. 2012; 148(5):1001–1014. [PubMed: 22385964]
33. Papadopoulou LC, Sue CM, Davidson MM, et al. Fatal infantile cardioencephalomyopathy with COX deficiency and mutations in SCO2, a COX assembly gene. Nat Genet. 1999; 23(3):333–337. [PubMed: 10545952]
34. Schambach A, Galla M, Modlich U, et al. Lentiviral vectors pseudotyped with murine ecotropic envelope: increased biosafety and convenience in preclinical research. Exp Hematol. 2006; 34(5): 588–592. [PubMed: 16647564]
35. Kiel MJ, Yilmaz OH, Iwashita T, et al. SLAM family receptors distinguish hematopoietic stem and progenitor cells and reveal endothelial niches for stem cells. Cell. 2005; 121(7):1109–1121. [PubMed: 15989959]
36. Oguro H, Ding L, Morrison SJ. SLAM family markers resolve functionally distinct subpopulations of hematopoietic stem cells and multipotent progenitors. Cell Stem Cell. 2013; 13(1):102–116. [PubMed: 23827712]
37. Yahata T, Takanashi T, Muguruma Y, et al. Accumulation of oxidative DNA damage restricts the self-renewal capacity of human hematopoietic stem cells. Blood. 2011; 118(11):2941–2950. [PubMed: 21734240]

38. Shimazu T, Hirschey MD, Newman J, He W, Shirakawa K, Le Moan N, et al. Suppression of oxidative stress by β-hydroxybutyrate, an endogenous histone deacetylase inhibitor. Science. 2013; 339(6116):211–4. [PubMed: 23223453]
39. Kawauchi K, Araki K, Tobiume K, Tanaka N. p53 regulates glucose metabolism through an IKKNF-κB pathway and inhibits cell transformation. Nat Cell Biol. 2008; 10:611–618. [PubMed: 18391940]
40. Meylan E, Dooley AL, Feldser DM, et al. Requirement for NF-κB signalling in a mouse model of lung adenocarcinoma. Nature. 2009; 462:104–107. [PubMed: 19847165]
41. Schwartzenberg-Bar-Yoseph F, Armoni M, Karnieli E. The tumor suppressor p53 down-regulates glucose transporters GLUT1 and GLUT4 gene expression. Cancer Res. 2004; 64:2627–2633. [PubMed: 15059920]
42. Kondoh H, Lleonart ME, Gil J, et al. Glycolytic enzymes can modulate cellular life span. Cancer Res. 2005; 65:177–185. [PubMed: 15665293]
43. Ide T, Brown-Endres L, Chu K, et al. GAMT, a p53-inducible modulator of apoptosis, is critical for the adaptive response to nutrient stress. Mol Cell. 2009; 36:379–392. [PubMed: 19917247]
44. Vousden KH. Alternative fuel-another role for p53 in the regulation of metabolism. Proc Natl Acad Sci USA. 2010; 107:7117–7118. [PubMed: 20393124]
45. Freie BW, Ciccone SL, Li X, et al. A role for the Fanconi anemia C protein in maintaining the DNA damage-induced G2 checkpoint. J Biol Chem. 2004; 279:50986–50993. [PubMed: 15377654]
46. Houghtaling S, Granville L, Akkari Y, et al. Heterozygosity for p53 (Trp53+/−) accelerates epithelial tumor formation in fanconi anemia complementation group D2 (Fancd2) knockout mice. Cancer Res. 2005; 65:85–91. [PubMed: 15665282]
47. Ceccaldi R, Briot D, Larghero J, et al. Spontaneous abrogation of the G_2DNA damage checkpoint has clinical benefits but promotes leukemogenesis in Fanconi anemia patients. J Clin Invest. 2011; 121(1):184–194. [PubMed: 21183791]
48. Ceccaldi R, Parmar K, Mouly E, et al. Bone marrow failure in Fanconi anemia is triggered by an exacerbated p53/p21 DNA damage response that impairs hematopoietic stem and progenitor cells. Cell Stem Cell. 2012; 11(1):36–49. [PubMed: 22683204]
49. Kohli L, Passegué E. Surviving change: the metabolic journey of hematopoietic stem cells. Trends Cell Biol. 2014; 24(8):479–487. [PubMed: 24768033]
50. TeKippe M, Harrison DE, Chen J. Expansion of hematopoietic stem cell phenotype and activity in Trp53-null mice. Exp Hematol. 2003; 31(6):521–527. [PubMed: 12829028]
51. Meng A, Wang Y, Van Zant G, Zhou D. Ionizing radiation and busulfan induce premature senescence in murine bone marrow hematopoietic cells. Cancer Res. 2003; 63(17):5414–5419. [PubMed: 14500376]
52. Wang Y, Schulte BA, Zhou D. Hematopoietic stem cell senescence and long-term bone marrow injury. Cell Cycle. 2006; 5(1):35–38. [PubMed: 16319536]
53. Chen J, Ellison FM, Keyvanfar K, et al. Enrichment of hematopoietic stem cells with SLAM and LSK markers for the detection of hematopoietic stem cell function in normal and Trp53 null mice. Exp Hematol. 2008; 36(10):1236–1243. [PubMed: 18562080]
54. Liu Y, Elf SE, Miyata Y, et al. p53 regulates hematopoietic stem cell quiescence. Cell Stem Cell. 2009; 4(1):37–48. [PubMed: 19128791]
55. Madan E, Gogna R, Bhatt M, et al. Regulation of glucose metabolism by p53: emerging new roles for the tumor suppressor. Oncotarget. 2011; 2(12):948–957. [PubMed: 22248668]

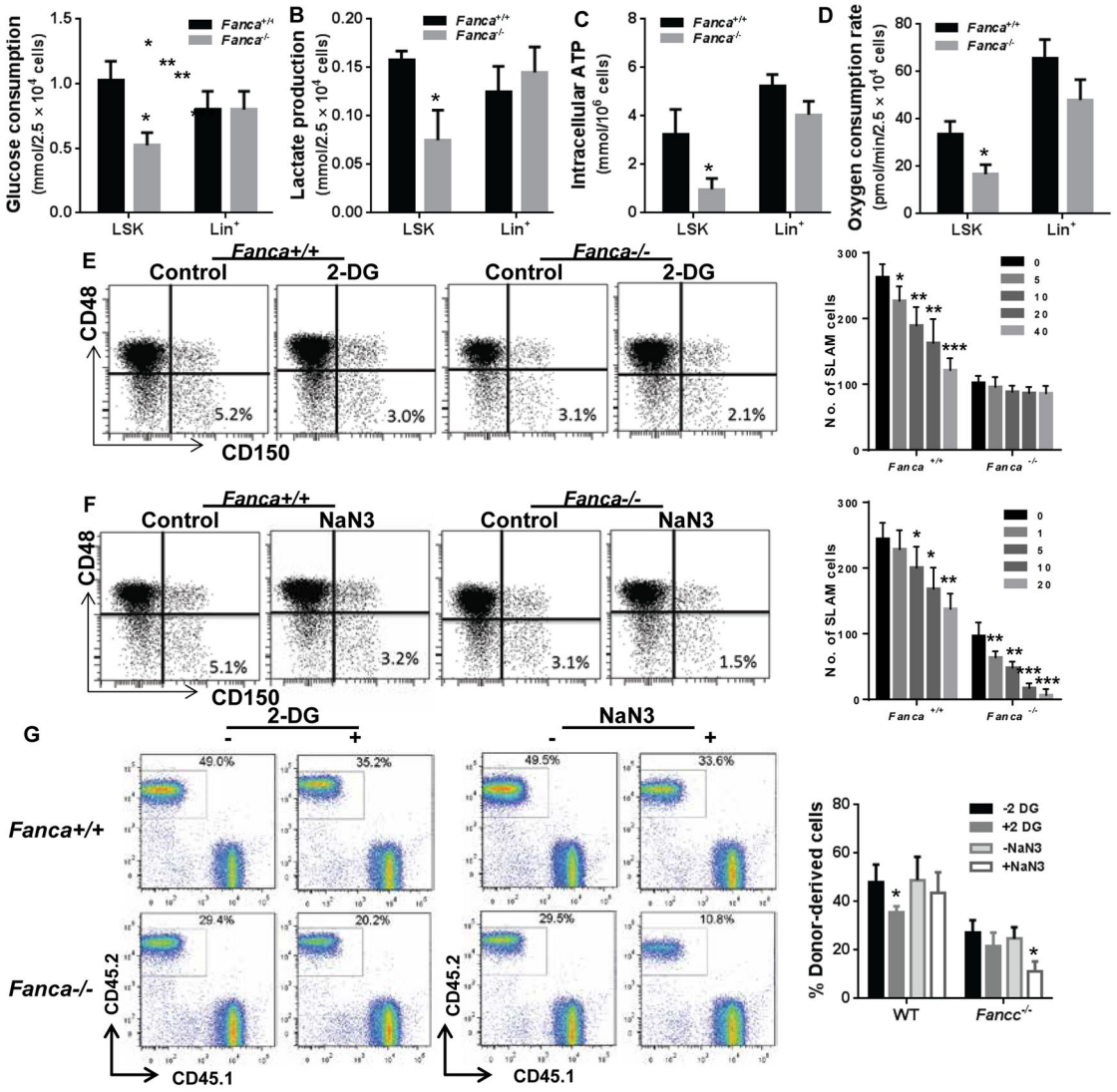

Fig 1. FA HSCs are more dependent on OXPHOS for energy metabolism

(A–B) Deletion of *Fanca* reduces glucose consumption and lactate production. LSK (Lin^- $Sca\text{-}1^+$ $c\text{-}Kit^+$) and Lin^+ cells from the bone marrow (BM) of wild-type (WT) or $Fanca^{-/-}$ mice were isolated by FACS and determined for glucose consumption (A) and lactate production (B). Results are means ± standard deviation (SD) of three independent experiments. (C) FA-deficient HSPCs produce lower ATP levels. Relative intracellular ATP concentrations were measured in LSK and Lin^+ cells. Results are means ± SD of three independent experiments. (D) FA HSPCs exhibit decreased oxygen consumption levels. Oxygen consumption rate (OCR) was measured in LSK and Lin^+ cells. Results are means ± SD of three independent experiments. (E) FA HSCs are resistant to the cytotoxicity of 2-DG. Low density bone marrow (LDBM) cells from WT and $Fanca^{-/-}$ mice were cultured in the presence of increasing concentrations of 2-DG for 12h and analyzed for the number of SLAM ($CD150^+CD48^-LSK$) cells. Shown are representative flow plots (left) for cells treated with 0 and 10mM 2-DG and quantification (right; number of SLAM cells per 10^6 LDBM cells) for cells treated with 0, 5, 10, 20 and 40mM 2-DG. Results are means ± SD of

3 independent experiments. (F) FA HSCs are hypersensitive to the cytotoxicity of the respiration inhibitor NaN3. LDBM cells from WT and *Fanca*$^{-/-}$ mice were cultured in the presence of increasing concentrations of NaN3 for 12h and analyzed for the number of SLAM cells. Shown are representative flow plots (left) for cells treated with 0 and 5mM NaN3 and quantification (right; number of SLAM cells per 10^6 LDBM cells) for cells treated with 0, 1, 5, 10, and 20mM NaN3. Results are means ± SD of 3 independent experiments. (G) Fifty SLAM cells from WT and *Fanca*$^{-/-}$ mice were treated with 0 and 10mM 2-DG or 0 and 5mM NaN3 for 12 h, mixed with 4×10^5 LDBM cells from recipient mice (CD45.2), and transplanted into lethally irradiated BoyJ congenic mice (CD45.2). Six months after transplantation, peripheral blood was collected and examined to determine the percentage of donor-derived cells by FACS. Representative flow plots (left) and quantification (right) are shown. Results are means ± SD of 3 independent experiments (n=12 per group). *$p < 0.05$.

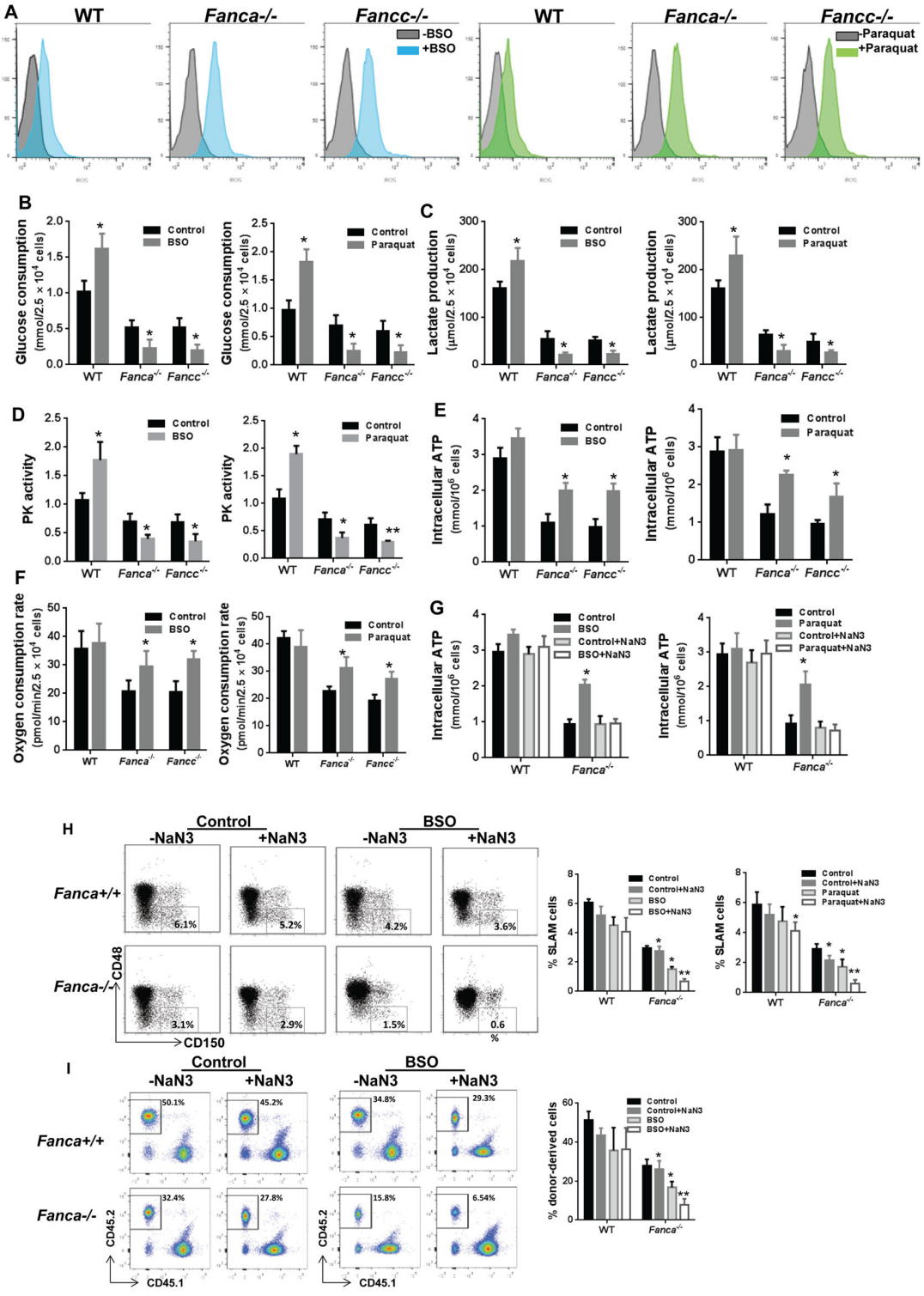

Fig 2. FA HSCs undergo glycolysis to OXPHOS switch in response to oxidative stress

(A) BSO and paraquat induce higher levels of ROS in *Fanca*$^{-/-}$ and *Fancc*$^{-/-}$ LSK cells than in WT LSK. WT, *Fanca*$^{-/-}$ and *Fancc*$^{-/-}$ LSK cells were treated with buthionine sulfoximine (BSO; 125µM) for 6 h or paraquat (100 µM) for 2 h, and labeled with CM-H2DCFDA for

Flow Cytometry analysis of ROS. Representative images are shown. (B–D) Decreased glucose consumption, lactate production and pyruvate kinase (PK) activity in oxidative stressed *Fanca*$^{-/-}$ LSK cells. WT and *Fanca*$^{-/-}$ LSK cells were treated with BSO (125μM) for 6 h or paraquat (100 μM) for 2 h, and determined for glucose consumption (B), lactate production (C), and PK activity (D). (E–F) Increased ATP production and mitochondria oxygen consumption in oxidative stressed *Fanca*$^{-/-}$ LSK cells. WT and *Fanca*$^{-/-}$ LSK cells were treated with 125μM BSO for 6 h or paraquat (100 μM) for 2 h, and determined for intracellular ATP levels (E) and oxygen consumption rate (F). (G) Inhibition of OXPHOS abrogates the elevated ATP synthesis induced by BSO in FA LSK cells. WT and *Fanca*$^{-/-}$ LSK cells were pre-treated with 5mM NaN3 for 30 min then with 125μM BSO for additional 6h or paraquat (100 μM) for additional 2 h, and determined for intracellular ATP levels. (H) OXPHOS inhibition further increases the sensitivity of *Fanca*$^{-/-}$ HSCs to oxidative stress. WT and *Fanca*$^{-/-}$ LDBM cells were pre-treated with 5mM NaN3 for 30 min then with 125μM BSO for additional 6h or paraquat (100 μM) for additional 2 h, and analyzed for the frequency of SLAM cells. Representative flow plots (left) and quantification (right) are shown. (I) OXPHOS inhibition further decreases the repopulating capacity of oxidative stressed *Fanca*$^{-/-}$ HSCs. Fifty SLAM cells from WT or *Fanca*$^{-/-}$ mice (CD45.2) were pre-treated with 5mM NaN3 for 30 min then with 125μM BSO for additional 6h, and transplanted together with 4×10^5 recipient cells into lethally irradiated BoyJ congenic mice. Representative flow plots (left) and quantification (right) are shown. (n=12 per group). *$p < 0.05$.

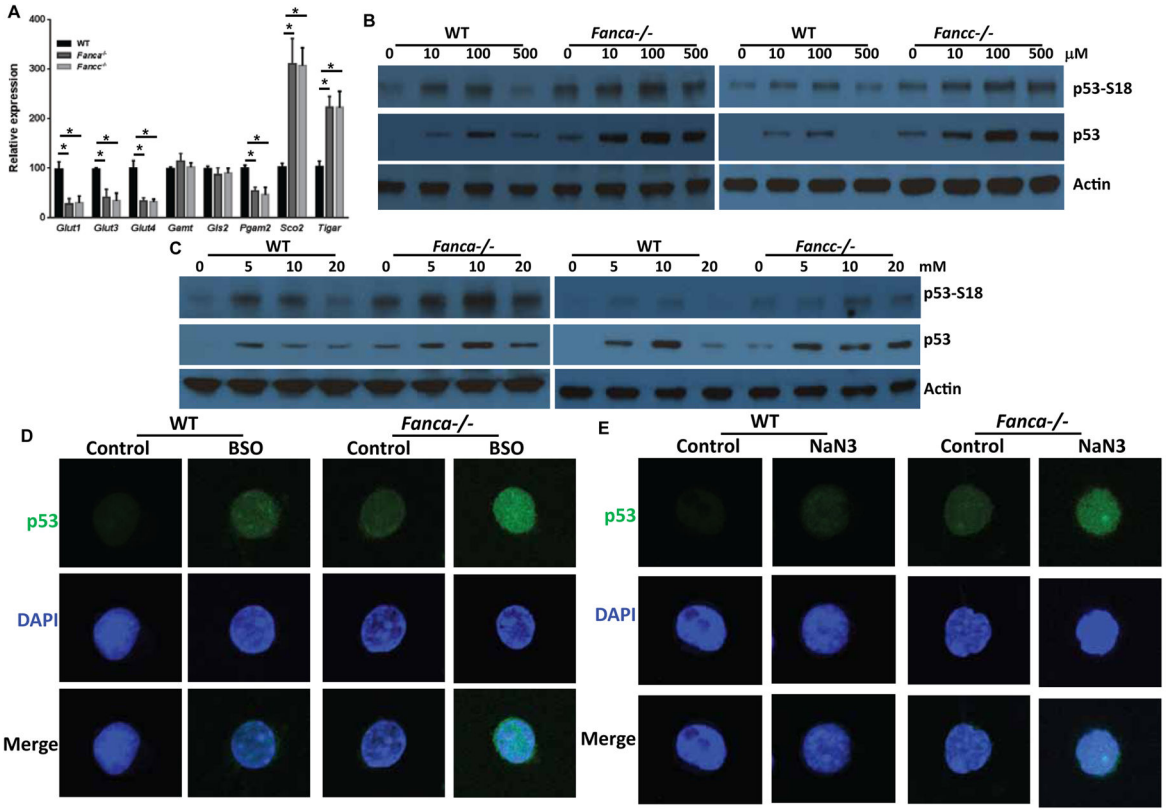

Fig 3. p53 is upregulated in FA HSCs in response to metabolic stress

(A) Deletion of *Fanca*$^{-/-}$ or *Fancc*$^{-/-}$ in SLAM cells upregulates basal and BSO-induced expression of p53 metabolic target genes. RNA were extracted from SLAM cells isolated from the BM of WT, *Fanca*$^{-/-}$, and *Fancc*$^{-/-}$ mice was used for real-time PCR analysis using primers specific for the indicated p53 target genes. Samples were normalized to the level of *GAPDH* mRNA. (B–C) *Fanca*$^{-/-}$ HSPCs display higher and prolonged p53 upregulation compared to WT cells in response to oxidative stress and OXPHOS inhibition. Lin^{-} cells isolated from WT and *Fanca*$^{-/-}$ mice were treated with increasing concentrations of BSO (B) or NaN3 (C) for 6 h, and cell lysates were subjected to immunoblot analysis using antibodies specific for the total p53, phosphorylated p53 (p53-S18) or β-actin. Each lane contains proteins from ~40,000 Lin^{-} cells. (D–E) p53 is overactivated in *Fanca*$^{-/-}$ HSCs in response to metabolic stress. Freshly isolated CD34^{-}LSK cells from WT and *Fanca*$^{-/-}$ BM were treated with 100μM BSO (D) or 10mM NaN3 (E) for 6h, and immunostained to detect p53 (green). Nuclei were visualized using 4′,6′-diamidino-2-phenylindole (DAPI; blue). Original magnification: ×60.

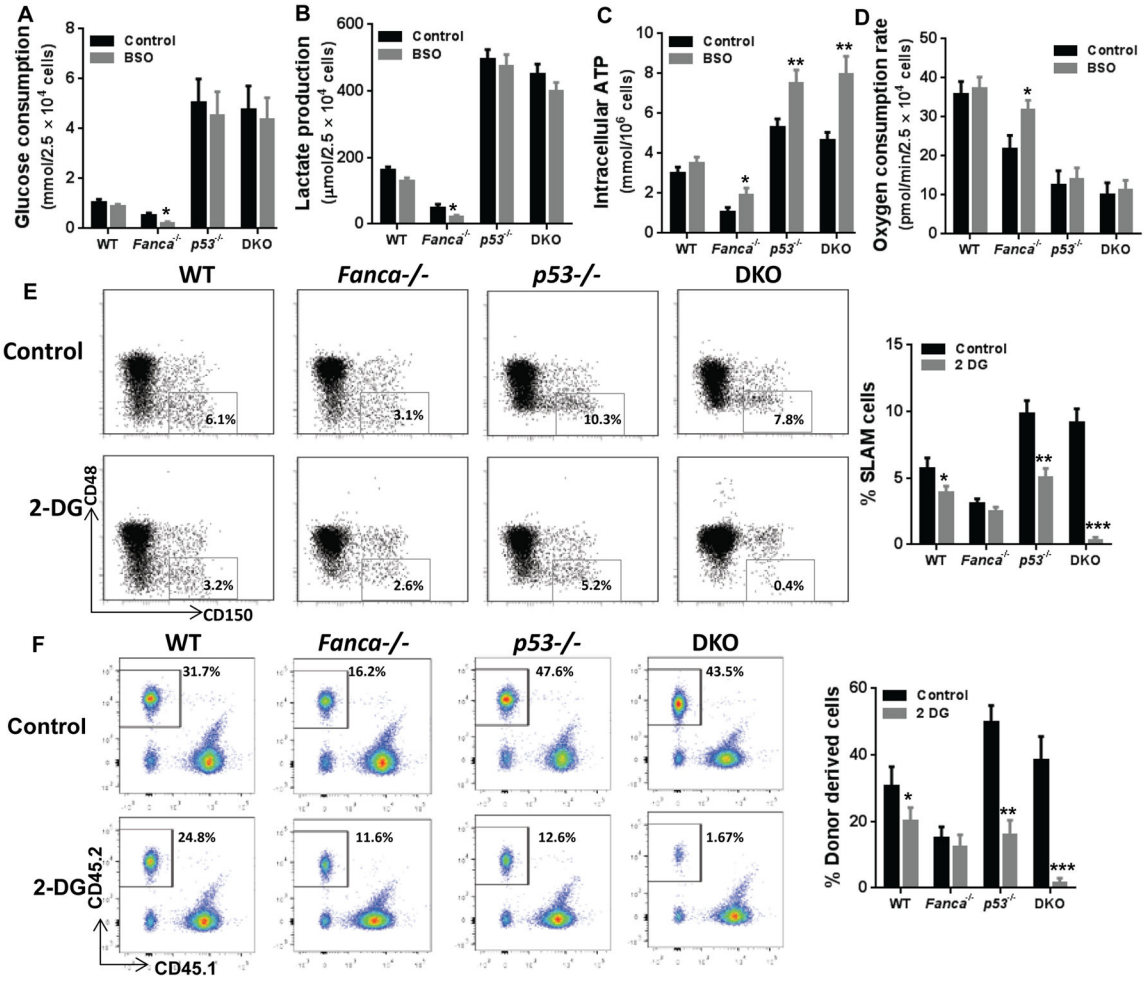

Fig 4. Oxidative stress mediates glycolysis to OXPHOS switch via p53 signaling

(A–B) Deletion of p53 increases glucose consumption and lactate production in HSCs. LSK cells isolated from WT, *p53*$^{-/-}$, *Fanca*$^{-/-}$ and *p53*$^{-/-}$*Fanca*$^{-/-}$ (DKO) were treated with 125μM BSO for 6 h, and determined for glucose consumption (A) and lactate production (B). (C) Deletion of p53 leads to increased ATP production in oxidative stressed *Fanca*$^{-/-}$ LSK cells. LSK cells isolated from WT, *p53*$^{-/-}$, *Fanca*$^{-/-}$ and *p53*$^{-/-}$*Fanca*$^{-/-}$ (DKO) were treated with 125μM BSO for 6 h, and determined for intracellular ATP production. (D) Oxidative stress decreases oxygen consumption in *p53*-deficient *Fanca*$^{-/-}$ LSK cells. LSK cells isolated from WT, *p53*$^{-/-}$, *Fanca*$^{-/-}$ and *p53*$^{-/-}$*Fanca*$^{-/-}$ (DKO) were treated with 125μM BSO for 6 h, and determined for oxygen consumption rate. (E) p53-deficient *Fanca*$^{-/-}$ HSCs are hypersensitive to glycolytic inhibition. LDBM cells from WT, *p53*$^{-/-}$, *Fanca*$^{-/-}$ and *p53*$^{-/-}$*Fanca*$^{-/-}$ (DKO) were treated with 10mM 2-DG for 12 h, and analyzed for the frequency of SLAM cells. Representative flow plots (left) and quantification (right) are shown. (F) Glycolytic inhibition further decreases the repopulating capacity of oxidative stressed *Fanca*$^{-/-}$ HSCs. 50 SLAM cells from WT, *p53*$^{-/-}$, *Fanca*$^{-/-}$ and *p53*$^{-/-}$*Fanca*$^{-/-}$ (DKO) were treated with 10mM 2-DG for 12 h, and then transplanted together with 4×10^5 recipient cells into lethally irradiated BoyJ congenic mice. Representative flow plots (left) and quantification (right) are shown. (n=9 per group). *$p < 0.05$.

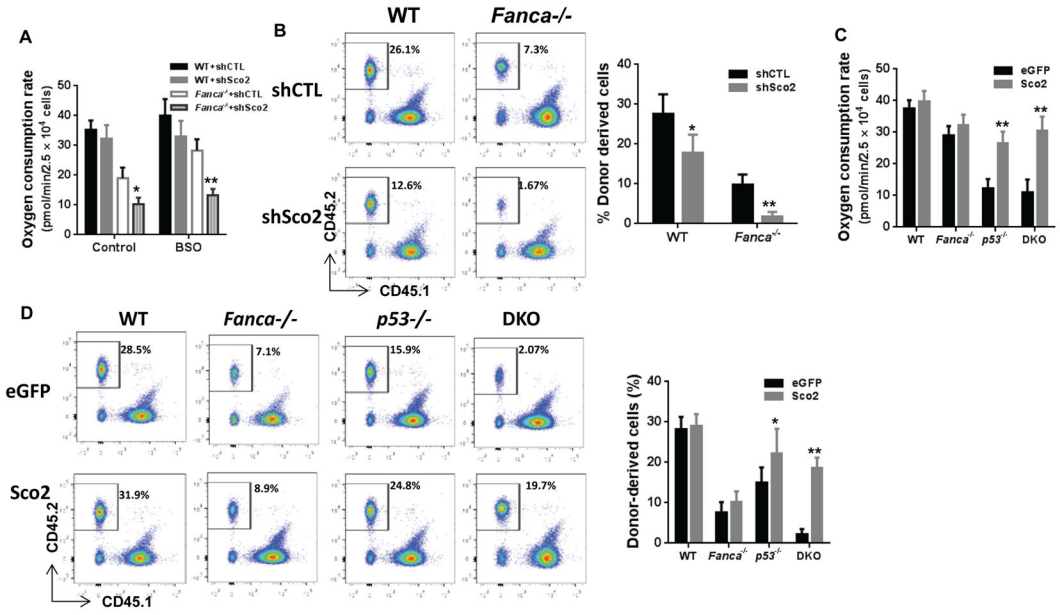

Fig 5. Oxidative stress-induced glycolysis to OXPHOS switch is mediated by SCO2

(A) Knocking down Sco2 reduces oxygen consumption in *Fanca*$^{-/-}$ LSK cells. BM LSK cells from WT and *Fanca*$^{-/-}$ mice were transduced with lentivirus encoding a control shRNA (shCTL) or a Sco2 shRNA (shSco2), treated with 125μM BSO for 6 h, and determined for oxygen consumption rate. (B) Knocking down Sco2 decreased repopulation of FA HSCs. 1,500 transduced WT or *Fanca*$^{-/-}$ LSK cells were treated with 125μM BSO for 6h, and then transplanted together with 4×10^5 recipient cells into lethally irradiated BoyJ congenic mice. Representative flow plots (left) and quantification (right) are shown. (n=6 per group). (C) Ectopic expression of SCO2 restores BSO-induced oxygen consumption of p53$^{-/-}$ or p53-deficient *Fanca*$^{-/-}$ LSK cells. BM LSK cells from WT, *p53*$^{-/-}$, *Fanca*$^{-/-}$ and *p53*$^{-/-}$*Fanca*$^{-/-}$ (DKO) were transduced with lentivirus expressing eGFP only (eGFP) or eGFP plus SCO2 (SCO2), treated with 125μM BSO for 6 h, and determined for oxygen consumption rate. (D) Ectopic expression of Sco2 rescues long-term hematopoietic repopulation of p53$^{-/-}$ or p53-deficient *Fanca*$^{-/-}$ LSK cells. 1,500 transduced WT, *p53*$^{-/-}$, *Fanca*$^{-/-}$ or *p53*$^{-/-}$*Fanca*$^{-/-}$ (DKO) LSK cells were treated with 125μM BSO for 6h, and then transplanted together with 4×10^5 recipient cells into lethally irradiated BoyJ congenic mice. Representative flow plots (left) and quantification (right) are shown. (n=6 per group). *$p < 0.05$.